

## Second-order self-energy–vacuum-polarization contributions to the Lamb shift in highly charged few-electron ions

Hans Persson and Ingvar Lindgren

*Department of Physics, Chalmers University of Technology and the University of Gothenburg, S-412 96 Göteborg, Sweden*

Leonti N. Labzowsky

*Department of Theoretical Physics, Petersburg State University, Ulianovskaya 1, Petrodvorets 198904, St. Petersburg, Russia*

Günter Plunien, Thomas Beier, and Gerhard Soff

*Institut für Theoretische Physik, Technische Universität Dresden, Mommsenstrasse 13, D-01062 Dresden, Federal Republic of Germany*

(Received 12 February 1996)

Proceeding towards the evaluation of the complete set of radiative corrections of order  $\alpha^2$  to the energy levels of hydrogenlike systems, the second-order self-energy–vacuum-polarization contribution to the Lamb shift of bound electrons is derived and calculated. We focus on the Uehling part of the vacuum-polarization insertion in the effective photon interaction. Additional energy corrections of order  $\alpha^2$  are also calculated. We present a brief summary of various energy contributions for *K*- and *L*-shell electrons in hydrogenlike and lithiumlike high-*Z* ions. [S1050-2947(96)12509-9]

PACS number(s): 31.10.+z, 31.30.Jv

### I. INTRODUCTION

During the last few years, a considerable improvement has been gained in precision measurements of the Lamb shift in highly charged few-electron ions. For Li-like uranium, the shift between the  $2s_{1/2}$  and the  $2p_{1/2}$  levels was measured to be  $280.59 \pm 0.09$  eV corresponding to a precision of  $3 \times 10^{-4}$  [1]. Measurements of the  $1s_{1/2}$  Lamb shift in H-like uranium increased in precision from  $520 \pm 130$  eV [2] to  $429 \pm 63$  eV achieved by Stöhlker *et al.* [3] and  $470 \pm 16$  eV measured by Beyer *et al.* [4] recently. An experimental error of 1 eV is reasonable in the near future [5].

This experimental success forces theoreticians to take into consideration the higher-order quantum electrodynamical (QED) corrections which contribute significantly at this level of precision. These corrections have to be calculated nonperturbatively in  $\alpha Z$  ( $\alpha$  is the fine-structure constant and  $Z$  is the nuclear charge number) since  $\alpha Z$  approaches unity for high  $Z$ . A variety of corresponding calculations have been performed during the last years for different first- and

second-order QED corrections, indicated in Figs. 1 and 2.

The first-order self-energy (SE) correction for high- $Z$  ions [Fig. 1(a)] has been calculated employing many different methods, beginning from the pioneering elaborations of Brown *et al.* [6] and Desiderio and Johnson [7] to the more accurate approach developed by Mohr [8,9]. Recently Blundell and Snyderman presented an alternative approach [10,11] of calculating the first-order self-energy also in a non-Coulomb potential and thus they could include two-

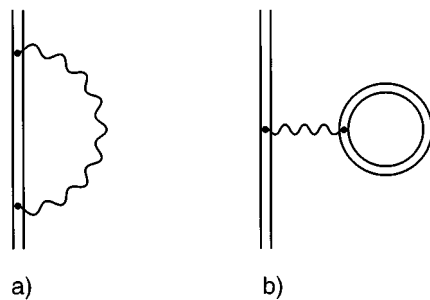


FIG. 1. Feynman graphs corresponding to QED corrections of first order in  $\alpha$ . The double solid line corresponds to the bound electron, and the wavy line to the photon.

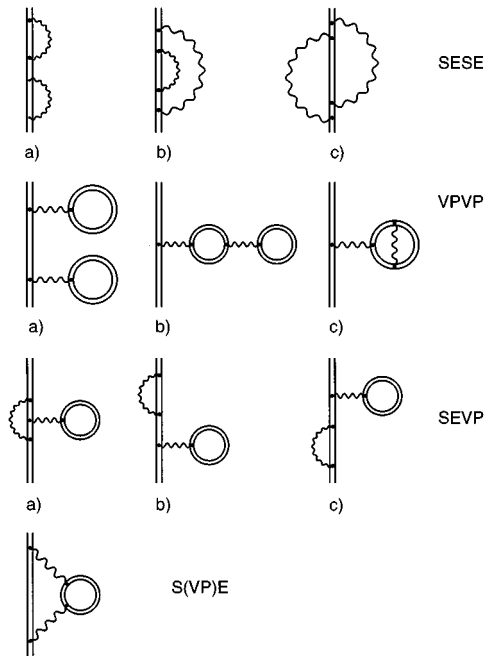


FIG. 2. Feynman graphs corresponding to the second-order QED corrections in one-electron ions. The notations are the same as in Fig. 1.

electron Lamb shift (electron screening) effects, by modifying the electron orbitals in the SE computation. All these methods are based on a nuclear potential expansion of the intermediate bound electron propagator in order to isolate analytically and to subtract the mass divergency. For higher-order QED corrections this procedure will be rather complicated. Later the method of the partial-wave renormalization (PWR) was developed (Persson *et al.* [12] and Quiney and Grant [13]), which appears to be rather promising for the higher-order QED calculations. This method has been applied to the electron-screened self-energy (SE) and to some of the combined self-energy–vacuum-polarization (SEVP) two-photon diagrams. This approach is based on a spherical-wave decomposition of the mass term in order to calculate the SE more directly without employing the potential expansion.

The first-order vacuum-polarization (VP) correction [Fig. 1(b)] can be divided into two major parts. The first is the charge divergent Uehling part which can be renormalized and calculated quite easily and the second, more difficult to elaborate, is the Wichmann-Kroll (WK) part. A good approximation of the Wichmann-Kroll part was first derived by Wichman and Kroll [14] and later a complete and accurate calculation was accomplished by Soff and Mohr [15]. The numerical accuracy in calculating the first-order VP has been further improved recently by Persson *et al.* [16]. Moreover, they have generalized their computational scheme to also incorporate electron-screening effects on the VP.

In addition to a complicated renormalization scheme, the calculation of higher-order QED corrections also requires the application of special numerical methods to perform the multiple summation over the complete bound-electron spectrum. The most frequently used numerical scheme is the *B*-spline method (Johnson *et al.* [17]) and the space discretization method (Salomonson and Oster [18]), used in [11,12] and [16].

Considering the one-particle two-photon QED effects, the second-order SESE, VPVP, SEVP, and S(VP)E corrections (see Fig. 2) represent separately gauge-invariant sets. The nondegenerate part (the irreducible part) of the SESE (a) correction in Fig. 2 was calculated by Mitrushenkov *et al.* [19] using a renormalization procedure similar to that of Snyderman [10] combined with the space discretization method. The remaining “reference” state part (see Labzowsky *et al.* [20]) of this diagram and the two SESE (b), (c) corrections in Fig. 2 are not yet calculated. The renormalization procedure for these remaining SESE corrections has recently been discussed by Labzowsky and Mitrushenkov [21] and by Lindgren [22].

The VPVP a correction in Fig. 2 was calculated by Persson *et al.* [16]. The idea was to solve the bound-electron Dirac equation for an extended nuclear charge distribution, with and without an additional VP potential. By subtracting the first-order VP correction from the difference in the bound-state eigenvalues the effect of the VPVP (a) diagram and higher-order vacuum-polarization effects could be extracted. In the present work this contribution was also recalculated using the same technique. Recently, the VPVP (a) correction has also been calculated by Manakov and Nekipelov [23] with the use of a point-nucleus Green function approach.

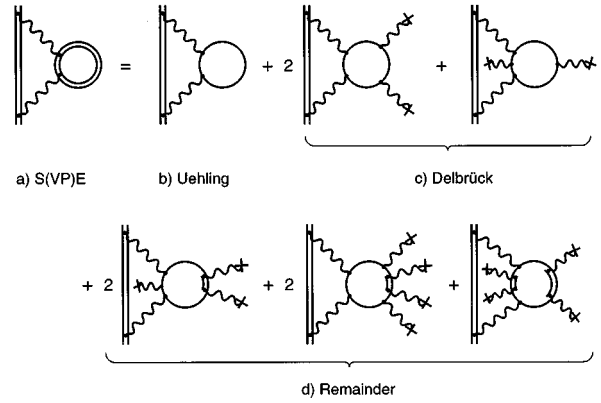


FIG. 3. Potential expansion of the vacuum polarization loop in the S(VP)E correction. The wavy line with the cross at the end denotes the interaction with the nuclear field. The ordinary single solid line denotes the free-electron propagator.

The two other VPVP corrections are known as Källén-Sabry contributions [24]. They were computed by Beier and Soff [25] and later by Schneider *et al.* [26] in the Uehling approximation. This approximation is usually valid for Coulomb-like VP corrections within the accuracy of a few percent [14–16].

The SEVP corrections were first elaborated on by Lindgren *et al.* [16,27], who included the vacuum polarization in the orbitals when calculating the first-order self-energy using PWR. By subtracting the ordinary first-order SE, the effect of the SEVP a),b),c) graphs was obtained. Note that this approach also takes into account automatically the reference-state corrections. In this work, this contribution has been recalculated with higher accuracy. The last remaining closed electron loop diagram, the S(VP)E correction, has not been evaluated up to now. The investigation of the Uehling part of S(VP)E is presented in this paper.

In addition to the second-order SE and VP contributions, the polarizability of the nucleus and the recoil effect due to its finite mass cause binding energy corrections of the same order of magnitude. The nuclear polarization was compiled by Plunien *et al.* [28,29]. The recoil effect to all orders in  $\alpha Z$  was derived recently by Artemyev *et al.* [30].

## II. THEORY

For the calculation of the S(VP)E correction, which is both charge and mass divergent, we shall employ the Uehling approximation. The potential expansion for the VP loop in the S(VP)E correction is depicted in Fig. 3. The first diagram of this expansion is charge divergent and after a standard charge renormalization we obtain the Uehling approximation that gives one part of the S(VP)E correction. We call this part S(VP)E1. The remaining diagrams, which we denote S(VP)E2, in Fig. 3 are not charge divergent even though special care has to be devoted to the spurious gauge dependent part of the Delbrück scattering term. The terms S(VP)E1 and S(VP)E2 have different orders of magnitude in the low-*Z* limit:  $(\alpha)^2(Z\alpha)^4 mc^2$  and  $(\alpha)^2(Z\alpha)^5 mc^2$  corre-

spondingly [31–33]. In our further derivations we restrict ourselves to the S(VP)E1 part. This part is also mass divergent and we shall use PWR to mass renormalize the S(VP)E1 correction.

First we recapitulate the main features of the PWR approach for the lowest-order self-energy, following Persson *et al.* [12]. The renormalized first-order bound-electron self-energy shift for a state  $\Phi_a(\mathbf{x}) = \langle \mathbf{x} | a \rangle$  can formally be written [8] as the real part of the bound self-energy and the mass counter term

$$\begin{aligned} \Delta E_{\text{bound}}^{\text{SE}}(a) = & \lim_{\Lambda \rightarrow \infty} \text{Re} \left\{ i e^2 \int d^3 x_2 \int d^3 x_1 \right. \\ & \times \int \frac{dz}{2\pi} \Phi_a^\dagger(\mathbf{x}_2) \alpha^\nu S_F(\mathbf{x}_2, \mathbf{x}_1, E_a - z) \alpha^\mu \Phi_a(\mathbf{x}_1) \\ & \times D_{F\nu\mu}^\Lambda(\mathbf{x}_2 - \mathbf{x}_1, z) \\ & \left. - \delta m(\Lambda) \int d^3 x \Phi_a^\dagger(\mathbf{x}) \beta \Phi_a(\mathbf{x}) \right\}, \quad (1) \end{aligned}$$

where  $S_F$  denotes the temporal Fourier transformed electron propagator. The corresponding covariant Pauli-Villars regulated photon propagator

$$\begin{aligned} D_{F\nu\mu}^\Lambda(\mathbf{x}_2 - \mathbf{x}_1, z) = & -g_{\nu\mu} \int \frac{d^3 k}{(2\pi)^3} e^{i\mathbf{k} \cdot (\mathbf{x}_2 - \mathbf{x}_1)} \\ & \times \left\{ \frac{1}{z^2 - \mathbf{k}^2 + i\epsilon} - \frac{1}{z^2 - \mathbf{k}^2 - \Lambda^2 + i\epsilon} \right\} \quad (2) \end{aligned}$$

is introduced in order to define a rigorous subtraction scheme that yields the correct Lorentz invariant shift. The lack of a simple analytical structure of the bound-electron propagator sets further constraints on how to cancel the divergencies in Eq. (1). To handle this, one usually performs a potential expansion of the bound-electron propagator into a free-electron propagator plus higher-order Coulomb scatterings. For the lowest-order self-energy this procedure was successfully applied by, for instance, Mohr [8,9]. However, its generalization to higher-order diagrams is not obvious. The po-

tential expansion procedure generates new charge divergencies which also have to be isolated and canceled.

In the PWR, an alternative approach is chosen. Start with the expression in Eq. (1), which can be written as

$$\Delta E_{\text{bound}}^{\text{SE}}(a) = \lim_{\Lambda \rightarrow \infty} \text{Re} \{ (B - B_\Lambda) - (M - M_\Lambda) \}, \quad (3)$$

where  $B$  and  $B_\Lambda$  are the two parts which result from a separation of the first term in Eq. (1) into a  $\Lambda$ -independent part and a  $\Lambda$ -dependent part of the regulated photon propagator in Eq. (2). The difference  $(M - M_\Lambda)$  is an alternative way of writing the regulated mass term given in Eq. (1).

Let us consider first the unrenormalized bound state SE, i.e., the  $B$  part. According to Eqs. (1) and (3) the corresponding expression reads

$$\begin{aligned} B = & i e^2 \int d^3 x_2 \int d^3 x_1 \int \frac{dz}{2\pi} \Phi_a^\dagger(\mathbf{x}_2) \\ & \times \alpha^\nu S_F(\mathbf{x}_2, \mathbf{x}_1, E_a - z) D_{F\nu\mu}(\mathbf{x}_2 - \mathbf{x}_1, z) \alpha^\mu \Phi_a(\mathbf{x}_1), \quad (4) \end{aligned}$$

where the time-independent unregulated photon propagator,  $D_{F\nu\mu}$ , and the time-independent electron propagator,  $S_F$ , have been introduced

$$S_F(\mathbf{x}_2, \mathbf{x}_1, z) = \sum_n \frac{\Phi_n(\mathbf{x}_2) \Phi_n^\dagger(\mathbf{x}_1)}{z - E_n(1 - i\eta)} = \frac{\langle \mathbf{x}_2 | n \rangle \langle n | \mathbf{x}_1 \rangle}{z - E_n(1 - i\eta)} \quad (5)$$

$$D_{F\nu\mu}(\mathbf{x}_2 - \mathbf{x}_1, z) = -g_{\nu\mu} \int \frac{d^3 k}{(2\pi)^3} \frac{e^{i\mathbf{k} \cdot (\mathbf{x}_2 - \mathbf{x}_1)}}{z^2 - \mathbf{k}^2 + i\epsilon}, \quad k = |\mathbf{k}|, \quad (6)$$

where the sum over  $n$  denotes a summation over positive and negative energy states. Evaluating the  $z$  integration by means of complex contour integration

$$\begin{aligned} & \int \frac{dz}{2\pi} \frac{1}{(z^2 - \mathbf{k}^2 + i\eta)} \frac{1}{[E_a - z - E_n(1 - i\eta')] } \\ & = - \frac{i}{2k[E_a - E_n - \text{sgn}(E_n)k]} \quad (7) \end{aligned}$$

we obtain

$$\begin{aligned} B = & -\alpha 2\pi \int d^3 x_2 \int d^3 x_1 \int \frac{d^3 k}{(2\pi)^3} \frac{1}{k} \sum_n \frac{\Phi_a^\dagger(\mathbf{x}_2) e^{i\mathbf{k} \cdot \mathbf{x}_2} \alpha_\mu \Phi_n(\mathbf{x}_2) \Phi_n^\dagger(\mathbf{x}_1) \alpha^\mu e^{-i\mathbf{k} \cdot \mathbf{x}_1} \Phi_a(\mathbf{x}_1)}{E_a - E_n - \text{sgn}(E_n)k} \\ & = -\frac{\alpha}{4\pi^2} \int d^3 k \frac{1}{k} \sum_n \frac{\langle a | \alpha_\mu e^{i\mathbf{k} \cdot \mathbf{x}_2} | n \rangle \langle n | e^{-i\mathbf{k} \cdot \mathbf{x}_1} \alpha^\mu | a \rangle}{E_a - E_n - \text{sgn}(E_n)k}. \quad (8) \end{aligned}$$

The angular part of the  $\mathbf{k}$  integration can be worked out next. Employing the standard spherical wave expansion

$$\frac{\sin[k|\mathbf{x}_2 - \mathbf{x}_1|]}{k|\mathbf{x}_2 - \mathbf{x}_1|} = \sum_{l=0}^{\infty} (2l+1) j_l(kr_1) j_l(kr_2) \mathbf{C}^l(1) \cdot \mathbf{C}^l(2), \quad (9)$$

where the dot product between the angular tensors implies

$$\mathbf{C}^l(2) \cdot \mathbf{C}^l(1) = \frac{4\pi}{2l+1} \sum_{m=-l}^l Y_{lm}(\Omega_2) Y_{lm}^*(\Omega_1), \quad (10)$$

we end up with the partial-wave decomposition for  $B$ :

$$\begin{aligned}
B &= \sum_{l=0}^{\infty} B^l \\
&= -\frac{\alpha}{\pi} \sum_{l=0}^{\infty} (2l+1) \int dk \frac{k^2}{k} \\
&\quad \times \sum_n \frac{\langle a | \alpha_{\mu} j_l(kr_2) \mathbf{C}^l | n \rangle \langle n | j_l(kr_1) \mathbf{C}^l \alpha^{\mu} | a \rangle}{E_a - E_n - \text{sgn}(E_n)k}. \quad (11)
\end{aligned}$$

Note that in Eq. (8), there is a logarithmic divergence in  $k$ . In Eq. (11) the divergency is moved from the  $k$  integration to the outer sum over partial waves. For each  $l$  value the  $k$  integration is finite. Thus, the partial-wave expansion serves as an effective cut-off. The  $B_{\Lambda}$  term can be worked out in an analogous way,

$$\begin{aligned}
B_{\Lambda} &= \sum_{l=0}^{\infty} B_{\Lambda}^l \\
&= -\frac{\alpha}{\pi} \sum_{l=0}^{\infty} (2l+1) \int dk \frac{k^2}{k'} \\
&\quad \times \sum_n \frac{\langle a | \alpha_{\mu} j_l(kr_2) \mathbf{C}^l | n \rangle \langle n | j_l(kr_1) \mathbf{C}^l \alpha^{\mu} | a \rangle}{E_a - E_n - \text{sgn}(E_n)k'}, \quad (12)
\end{aligned}$$

where  $k' = \sqrt{k^2 + \Lambda^2}$ .

---


$$\begin{aligned}
M &= \sum_{l=0}^{\infty} M^l \\
&= -\frac{\alpha}{\pi} \sum_{l=0}^{\infty} (2l+1) \sum_{r,r',s} \int d^3p \int d^3p' \int d^3q \int dk \frac{k^2}{k} \langle a | \mathbf{p}, r \rangle \frac{\langle \mathbf{p}, r | \alpha_{\mu} j_l(kr_2) \mathbf{C}^l | \mathbf{q}, s \rangle \langle \mathbf{q}, s | j_l(kr_1) \mathbf{C}^l \alpha^{\mu} | \mathbf{p}', r' \rangle}{E_{p,r} - E_{q,s} - \text{sgn}(E_{q,s})k} \langle \mathbf{p}', r' | a \rangle. \quad (15)
\end{aligned}$$

The  $M_{\Lambda}$  term looks similar to the  $M$  term in Eq. (15) and can be identified directly by replacing  $k$  by  $k'$  in the denominators as in Eq. (12). There are, however, ambiguities concerning the uniqueness of this mass term. The mass term is naturally associated with the mass in the Dirac equation and therefore proportional to  $\beta$ . The mass term given in Eq. (14) has the disadvantage of not being explicitly proportional to  $\beta$ . This is a well-known problem that was discussed extensively in the early days of QED. To justify the use of Eq. (14), it is explicitly shown in [35] that the partial-wave mass term in Eq. (14) is identical to the standard one.

By using the above derived expressions in the partial-wave form and since the  $l$ -dependent part of the photon propagator can be factored out, we can write the self-energy as

We now turn to the second part of Eq. (1), i.e., the bound-state mass counter term. This term is defined as the free-electron self-energy calculated for a momentum distribution determined by the bound state (French and Weisskopf [34]). We start with the expression for the free-electron self-energy in Feynman gauge, which is analogous to Eq. (8),

$$\begin{aligned}
\Delta E_{\text{free}}^{\text{SE}}(\mathbf{p}, r) &= -\alpha \frac{1}{4\pi^2} \int d^3k \frac{1}{k} \int d^3q \\
&\quad \times \sum_s \frac{\langle \mathbf{p}, r | \alpha_{\mu} e^{i\mathbf{k} \cdot \mathbf{x}_2} | \mathbf{q}, s \rangle \langle \mathbf{q}, s | e^{-i\mathbf{k} \cdot \mathbf{x}_1} \alpha^{\mu} | \mathbf{p}, r \rangle}{E_{p,r} - E_{q,s} - \text{sgn}(E_{q,s})k}, \quad (13)
\end{aligned}$$

where the ket  $|\mathbf{p}, r\rangle$  describes the free-electron state with the momentum  $\mathbf{p}$  and spin projection  $r$ , i.e.,  $\psi_{p,r}(\mathbf{x}) = \langle \mathbf{x} | \mathbf{p}, r \rangle$ .

Taking the free-electron self-energy sandwiched between the bound-state momentum distribution, we can express the mass term in the following form:

$$\begin{aligned}
M &= -\alpha \frac{1}{4\pi^2} \sum_{r,r',s} \int d^3p \int d^3p' \int d^3q \int d^3k \frac{1}{k} \langle a | \mathbf{p}, r \rangle \\
&\quad \times \frac{\langle \mathbf{p}, r | \alpha_{\mu} e^{i\mathbf{k} \cdot \mathbf{x}_2} | \mathbf{q}, s \rangle \langle \mathbf{q}, s | e^{-i\mathbf{k} \cdot \mathbf{x}_1} \alpha^{\mu} | \mathbf{p}', r' \rangle}{E_{p,r} - E_{q,s} - \text{sgn}(E_{q,s})k} \langle \mathbf{p}', r' | a \rangle \quad (14)
\end{aligned}$$

or in the partial-wave form which is analogous to Eq. (11),

---


$$\Delta E_{\text{bound}}^{\text{SE}}(a) = \lim_{\Lambda \rightarrow \infty} \text{Re} \left\{ \sum_{l=0}^{\infty} B^l - B_{\Lambda}^l - M^l + M_{\Lambda}^l \right\} \quad (16)$$

or since every term is finite we can reorder them to yield

$$\Delta E_{\text{bound}}^{\text{SE}}(a) = \text{Re} \left\{ \sum_{l=0}^{\infty} (B^l - M^l) - \lim_{\Lambda \rightarrow \infty} \sum_{l=0}^{\infty} (B_{\Lambda}^l - M_{\Lambda}^l) \right\}. \quad (17)$$

The correction term, the last part of the above expression can be shown to be zero when the limit  $\Lambda \rightarrow \infty$  is taken [34]. This is not always the case in higher-order effects and for in-

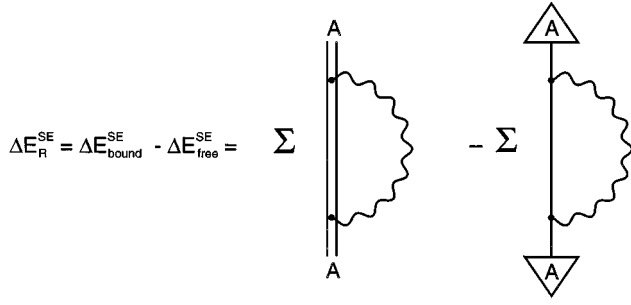


FIG. 4. Graphical representation of the renormalization procedure for the self-energy correction in PWR approach. Here  $A$  denotes the bound-electron state. The triangles denote the Fourier expansion of the state  $A$  in terms of plane waves. The summation represents the partial-wave expansion. The parts  $\Delta E_{\text{bound}}^{\text{SE}}$  and  $\Delta E_{\text{free}}^{\text{SE}}$  correspond to the bound and free electrons and  $\Delta E_R^{\text{SE}}$  is the renormalized electron self-energy correction.

stance, for the self-energy in an external magnetic field the correction term gives rise to a finite shift [34].

In summary, the partial-wave renormalization procedure for the first-order self-energy can be written as

$$\begin{aligned} \Delta E_R^{\text{SE}}(a) &= \text{Re} \left\{ \sum_{l=0}^{\infty} (B^l - M^l) \right\} \\ &= -\frac{\alpha}{\pi} \sum_{l=0}^{\infty} (2l+1) \text{Re} \left\{ \int dk k \right. \\ &\quad \times \sum_n \frac{\langle a | \alpha_{\mu} j_l(kr_2) \mathbf{C}^l | n \rangle \langle n | j_l(kr_1) \mathbf{C}^l \alpha^{\mu} | a \rangle}{E_a - E_n - \text{sgn}(E_n)k} \\ &\quad \left. - \sum_{r,r',s} \int d^3p \int d^3p' \int d^3q \int dk k \langle a | \mathbf{p}, r \rangle \right\} \end{aligned}$$

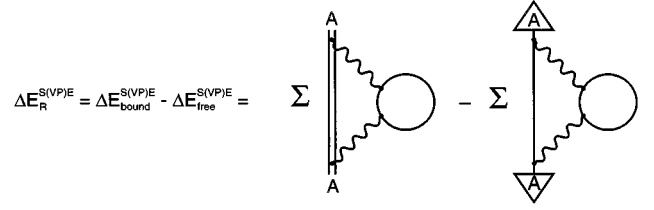


FIG. 5. Graphical representation of the renormalization procedure for the mixed self-energy-vacuum-polarization correction in PWR approach. The notations are the same as in Fig. 4.

$$\begin{aligned} \Delta E_R^{\text{S(VP)E}} &= \Delta E_{\text{bound}}^{\text{S(VP)E}} - \Delta E_{\text{free}}^{\text{S(VP)E}} = \sum \\ &\quad \times \frac{\langle \mathbf{p}, r | \alpha_{\mu} j_l(kr_2) \mathbf{C}^l | \mathbf{q}, s \rangle \langle \mathbf{q}, s | j_l(kr_1) \mathbf{C}^l \alpha^{\mu} | \mathbf{p}', r' \rangle}{E_{p,r} - E_{q,s} - \text{sgn}(E_{q,s})k} \\ &\quad \times \langle \mathbf{p}', r' | a \rangle \}. \end{aligned} \quad (18)$$

Graphically the PWR procedure can be represented as displayed in Fig. 4.

Comparing the graphs in Figs. 1(a) and 3(b) we can observe that they differ only by changing the usual photon propagator in Fig. 1(a) to the ‘‘effective’’ photon propagator in Fig. 3(b). We can use the known renormalized expression for the first-order polarization function leading to the following expression for the Fourier transform of the ‘‘effective’’ propagator (see, for example, Bogoljubov and Shirkov [36]):

$$\tilde{D}_{F\mu\nu}^{\Lambda}(k^2) = \frac{\alpha}{\pi} I(k^2) D_{F\mu\nu}^{\Lambda}(k^2), \quad (19)$$

$$I(k^2) = -k^2 \int_0^1 \frac{dv v^2 \left(1 - \frac{1}{3}v^2\right)}{4m^2 - i\epsilon' - k^2(1-v^2)}, \quad (20)$$

TABLE I. Different two-photon closed electron-loop energy contributions to the  $1s_{1/2}$  state for various hydrogenlike high- $Z$  ions. The second column relates our terminology to the notation used by Pachucki. Our numerical values (Num) are compared to the recently derived ( $Z\alpha$ ) expansions ( $Z\alpha$ -ex) which are correct to order  $(\alpha)^2(Z\alpha)^5 mc^2$ . All values are given in eV.

$Z$		70		82		92	
$\langle r^2 \rangle^{1/2}$		5.41 fm		5.50 fm		5.86 fm	
Diagram		$Z\alpha$ -ex	Num	$Z\alpha$ -ex	Num	$Z\alpha$ -ex	Num
VPVP(a)	VI(1)	-0.006	-0.025	-0.013	-0.083	-0.024	-0.217
VPVP(b),(c)	IV+VI(2)	-0.049	-0.185	-0.047	-0.393	-0.015	-0.716
SEVP	III	0.184	0.206	0.406	0.534	0.722	1.139
S(VP)E1	II	0.005	0.030	0.002	0.068	-0.007	0.130
S(VP)E2	V	-0.037		-0.082		-0.145	
Sum		0.097	0.026	0.266	0.126	0.531	0.336

where  $k^2 = z^2 - \mathbf{k}^2$ . Then the time-independent unregularized propagator  $\widetilde{\mathcal{D}}_{F\nu\mu}(\mathbf{x}_2, \mathbf{x}_1, z)$  can be presented in the form

$$\begin{aligned} \widetilde{\mathcal{D}}_{F\nu\mu}(\mathbf{x}_2 - \mathbf{x}_1, z) &= \frac{\alpha}{\pi} g_{\mu\nu} \int \frac{d^3k}{(2\pi)^3} e^{ik \cdot (\mathbf{x}_2 - \mathbf{x}_1)} \\ &\times \int_0^1 \frac{dv v^2 \left(1 - \frac{1}{3} v^2\right)}{(1-v^2) \left(\frac{4m^2 - i\epsilon'}{1-v^2} - z^2 + \mathbf{k}^2\right)}. \end{aligned} \quad (21)$$

The basic idea is now to cast the renormalized expression for  $\Delta E_R^{\text{S(VP)E1}}(a)$  in a form which is analogous to the  $\Delta E_R^{\text{SE}}$  expression. We consider first the analogous  $B$  part which can be written as

$$\begin{aligned} \Delta E_R^{\text{S(VP)E1}}(a) &= \text{Re} \left\{ \sum_{l=0}^{\infty} (B_l^{\text{S(VP)E1}} - M_l^{\text{S(VP)E1}}) \right\} \\ &= -\frac{\alpha^2}{\pi^2} \sum_{l=0}^{\infty} (2l+1) \text{Re} \left\{ \int dk k^2 \sum_n \langle a | \alpha_{\mu} j_l(kr_2) \mathbf{C}^l | n \rangle \langle n | j_l(kr_1) \mathbf{C}^l \alpha^{\mu} | a \rangle \right. \\ &\times \int_0^1 \frac{dv v^2 (1 - \frac{1}{3} v^2)}{\sqrt{4m^2 + k^2 (1-v^2)} [(E_a - E_n) \sqrt{1-v^2} - \sqrt{4m^2 + k^2 (1-v^2)} \text{sgn} E_n]} - \sum_{r, r', s} \int d^3p \int d^3p' \int dk k^2 \\ &\times \sum_q \langle a | p, r \rangle \langle p, r | \alpha_{\mu} j_l(kr_2) \mathbf{C}^l | q, s \rangle \langle q, s | j_l(kr_1) \mathbf{C}^l \alpha^{\mu} | p', r' \rangle \\ &\times \left. \int_0^1 \frac{dv v^2 (1 - \frac{1}{3} v^2)}{\sqrt{4m^2 - k^2 (1-v^2)} [(E_{p,r} - E_{q,s}) \sqrt{1-v^2} - \sqrt{4m^2 + k^2 (1-v^2)} \text{sgn} E_{q,s}]} \right\}. \end{aligned} \quad (25)$$

The diagrammatic representation of the PWR indicated by this equation is depicted in Fig. 5. Unlike the first-order self-energy [Fig. 1(a)], it can be shown explicitly that the expression inside the Re parenthesis in Eq. (25) generates no imaginary part for excited states. Accordingly, the process given by diagram Fig. 3(b) does not contribute to the line-width of excited electron states.

### III. NUMERICAL RESULTS AND DISCUSSION

For the S(VP)E1 contribution, the angular and radial integration in Eqs. (14), (15) can be performed by following the lines given in [8] with one extra integration over the parameter  $v$ . The results for this effect and the other closed electron-loop effects for the  $1s_{1/2}$  state in some hydrogenlike high- $Z$  ions are shown in Table I. For all contributions a homogeneously charged nucleus of the specified radius is employed. All values were recalculated here except those of

$$\begin{aligned} B^{\text{S(VP)E1}} &= i e^2 \int d^3x_2 \int d^3x_1 \int \frac{dz}{2\pi} \Phi_a^+(\mathbf{x}_2) \\ &\times \alpha^{\nu} S(\mathbf{x}_2, \mathbf{x}_1, E_a - z) \widetilde{\mathcal{D}}_{F\nu\mu}(\mathbf{x}_2 - \mathbf{x}_1, z) \alpha^{\mu} \Phi_a(\mathbf{x}_1). \end{aligned} \quad (22)$$

By using the expressions for the propagators [Eqs. (2) and (21)] the integration over  $z$  can be performed. Denoting

$$K^2 \equiv \frac{4m^2}{1-v^2} + \mathbf{k}^2 \quad (23)$$

we get

$$\begin{aligned} &\int \frac{dz}{2\pi} \frac{1}{[E_a - E_n(1-i\eta) - z]} \frac{1}{K^2 - z^2 - i\epsilon} \\ &= \frac{i}{2K} \frac{1}{E_a - E_n - K \text{sgn} E_n}. \end{aligned} \quad (24)$$

Including also the corresponding mass counter term, this can be written in the same form as Eq. (18),

the VPVP b),c) contributions, which are taken from [26]. In this table we also give a comparison with the leading terms in the  $(Z\alpha)$ -expansion, correct to order  $\alpha^2(Z\alpha)^5 mc^2$ , for the different closed electron-loop effects [31–33]. Considering the  $(Z\alpha)$ -expansion result, it can be noted that the only contributions of order  $\alpha^2(Z\alpha)^4 mc^2$  come from the S(VP)E1 [31] and the VPVP c) [37,38] diagrams.

Even though the calculation of closed electron-loop effects is not complete, it is interesting to note that the different effects [S(VP)E1, SEVP, and VPVP] are numerically significant but cancel to a large extent when added. As expected, there is also a substantial deviation if one compares our numerical values with the  $(Z\alpha)$ -expansion results. The difference is due to our inclusion of higher-order terms in  $(Z\alpha)$ , nuclear-size effects and relativistic effects. To complete the closed electron-loop effects one has to calculate the S(VP)E2 effect and higher-order in  $(Z\alpha)$  Källén-Sabry contributions. Both these missing effects can hopefully be cal-

TABLE II. Binding energies and first- and second-order QED corrections of  $1s_{1/2}$ ,  $2s_{1/2}$ , and  $2p_{1/2}$  electrons in H-like uranium ( $Z=92$ ). All values are given in eV.

		$1s_{1/2}$	$2s_{1/2}$	$2p_{1/2}$	Reference
Binding energy $E_B$ for point nucleus:		-132279.96	-34215.49	-34215.49	
Correction	Order				
Finite size		198.82	37.77	4.42	[39]
– Uehling		-93.58	-16.46	-2.90	[16]
– WK		4.99	0.82	0.21	[16]
Total VP	$m\alpha(\alpha Z)^4$	-88.60	-15.64	-2.70	
SE	$m\alpha(\alpha Z)^4$	355.05	65.42	9.55	[40,41]
SESE a) (irr)	$m\alpha^2(\alpha Z)^5$	-0.97	-0.08	0.01	[19]
SESE a) (red) + SESE b),c)	$m\alpha^2(\alpha Z)^4$	remain to be compiled			
VPVP a)	$m\alpha^2(\alpha Z)^5$	-0.22	-0.04	0.00	[16], This work
VPVP b),c)	$m\alpha^2(\alpha Z)^4$	-0.72	-0.12	-0.02	[25]
SEVP a)-c)	$m\alpha^2(\alpha Z)^5$	1.14	0.21	0.02	[27], This work
S(VP)E	$m\alpha^2(\alpha Z)^4$	0.13	0.02	0.00	This work
Recoil	$\frac{m}{M}(\alpha Z)^2$	0.51	0.13	0.09	[30,38]
Nuclear pol.	$\frac{m}{M}(\alpha Z)^2$	-0.18	-0.03	0.00	[28,29]
Sum of corrections		464.96	87.64	11.37	
Total binding energy		-131815.00	-34127.85	-34204.12	
Reduced mass	$\frac{m}{M}(\alpha Z)^2$	0.30	0.08	0.08	
Lamb shift (Theory)		464.66	87.56	11.29	
Lamb shift (Expt.)		470	(16)		[4]

culated soon, but the major difficulty are the remaining SESE effects.

The numerical results for the lowest-lying states in hydrogenuke uranium  $U^{91+}$  are given in Table II, which displays all first- and second-order QED corrections to the Dirac binding energy in the field of a point nucleus. The finite-size correction is obtained assuming a Fermi distribution with  $\langle r^2 \rangle^{1/2} = 5.860$  fm for the nuclear charge distribution. The absolute difference between the binding energy obtained for a homogeneously charged sphere and that for the Fermi distribution with the same rms radius implies an estimate for an uncertainty, which merely amounts to 0.36 eV. For details we refer to Ref. [39]. All first-order corrections presented here were obtained utilizing a uniform sphere model for the nuclear charge distribution. For the fundamental constants we employed the values  $1/137.036$  for  $\alpha$ , 386.159323 fm for the electron Compton wavelength, and 510999.06 eV for the electron rest mass. The self-energy was compiled according to the methods described in [40] and [41]. Minor important modifications are caused by different values of nuclear radii employed in the calculation. Also the VPVP a) contribution was reevaluated. Its values have also been confirmed utilizing the Wichmann-Kroll charge density compiled by Soff and Mohr [15]. Although they employed a spherical shell model for the nuclear charge distribution, no difference between the compilations occurred at the considered level of precision. The recoil correction [30] includes both reduced mass and relativistic recoil corrections. Note that it amounts

to 0.51 eV when using the more precise values of Table I in [30] instead of 0.50 eV due to the contributions stated explicitly in that article.

The Lamb shift for a single energy level by convention [42] includes all corrections beyond the point nucleus Dirac eigenvalue except the non-relativistic reduced mass correction and contributions due to hyperfine structure. The reduced mass correction is given by  $-m/(m+M)E_B$ , where  $M$  is the nuclear mass and  $E_B$  denotes the Dirac point-nucleus binding energy. To obtain the proper Lamb shift, this correction has to be subtracted from the sum of corrections. In the end of Table II we compare our theoretical values for the Lamb shift with the most recent corresponding experimental value [4] for the ground state of uranium.

In Table III we display the result for the  $2p_{1/2}-2s_{1/2}$  transition in lithiumlike uranium  $U^{89+}$ . The first line of Table III corresponds to the relativistic many-body perturbation theory calculation. This calculation differs from the full QED result, which is still absent, by the following details: in RMBPT there are (1) no retardation, (2) no virtual pairs (i.e. no negative energy intermediate states), and (3) no cross-photon Feynman graphs. The rough estimate of these corrections leads to the possible error given in the first line of Table III. The small two-photon reference-state corrections, also absent in RMBPT, are given separately. The nuclear size corrections are included in RMBPT, as well as in SE, VP, and corresponding screening corrections. However, the uncertainty in the nuclear size correction, obtained from the

TABLE III.  $2p_{1/2}-2s_{1/2}$  shift in Li-like U.

Correction	Order of magnitude and scaling	Numerical value (eV)	Reference
RMBPT	$m\alpha(\alpha Z)$	322.33(15)	Lindgren <i>et al.</i> [12,27]
SE	$m\alpha(\alpha Z)^4$	-55.87	Lindgren <i>et al.</i> [12]
SE screening	$m\alpha^2(\alpha Z)^3$	1.55	Lindgren <i>et al.</i> [12]
VP	$m\alpha(\alpha Z)^4$	12.94	Persson <i>et al.</i> [16]
VP screening	$m\alpha^2(\alpha Z)^3$	-0.39	Persson <i>et al.</i> [16]
SESE a) (irr)	$m\alpha^2(\alpha Z)^5$	0.09	Mitrushenkov <i>et al.</i> [19]
SEVP	$m\alpha^2(\alpha Z)^5$	-0.19	Lindgren <i>et al.</i> [27]
S(VP)E	$m\alpha^2(\alpha Z)^5$	-0.02	This work
VPVP a)	$m\alpha^2(\alpha Z)^5$	0.03	This work, Persson <i>et al.</i> [16]
VPVP b),c)	$m\alpha^2(\alpha Z)^4$	0.10	Schneider, Greiner, and Soff [25]
Two-photon reference state (box)	$m\alpha^2(\alpha Z)^3$	0.04	Lindgren <i>et al.</i> [27]
Two-photon reference state (cross)	$m\alpha^2(\alpha Z)^3$	-0.02	Labzowsky and Tokman [44]
Recoil	$\frac{m}{M}(\alpha Z)^2$	-0.08	Artemyev <i>et al.</i> [30], Blundell [45]
Nuclear polarization	$\frac{m}{M}(\alpha Z)^2$	0.03	Plunien <i>et al.</i> [28,29]
Total theory		280.54(15)	
Experiment		280.59(9)	Schweppe <i>et al.</i> [1]

results of Ynnerman *et al.* [43], which amounts to 0.03 eV, appears to be of the same order of magnitude as the second order QED corrections.

The analysis based on the Table III leads to the conclusions that the further refinement of the  $2p_{1/2}-2s_{1/2}$  energy shift calculation for hydrogenlike uranium requires first the full QED calculation of one- and two-photon exchange graphs and second the reduction of the nuclear size uncertainty. We should emphasize that the nuclear polarization and recoil have to be taken into account on this level of accuracy.

*Note added.* Recently we received a copy of unpublished work [46] by S. Mallampalli and J. Sapirstein on the same

subject. We are grateful for making their results available to us prior to publication.

#### ACKNOWLEDGMENTS

Peter J. Mohr and Sten Salomonson are greatly acknowledged for valuable discussions concerning the manuscript. The authors gratefully acknowledge financial support from various institutions: H.P. and I.L. acknowledge support from the Alexander von Humboldt foundation and L.L. acknowledges support by the REHE program. G.P., Th.B., and G.S. also acknowledge support by the BMBF, by the DFG, and by GSI (Darmstadt).

- 
- [1] J. Schweppe, A. Belkacem, L. Blumenfeld, N. Claytor, B. Feinberg, H. Gould, V. E. Costram, L. Levy, S. Misawa, J. R. Mowat, and M. H. Prior, *Phys. Rev. Lett.* **66**, 1434 (1991).
- [2] J. P. Briand, P. Chevallier, P. Indelicato, K. P. Ziock, and D. D. Dietrich, *Phys. Rev. Lett.* **65**, 2761 (1990).
- [3] Th. Stöhlker, P. H. Mokler, K. Beckert, F. Bosch, H. Eickhoff, B. Franzke, M. Jung, T. Kandler, O. Klepper, C. Kozhuharov, R. Moshhammer, F. Nolden, H. Reich, P. Rymuza, P. Spädtke, and M. Steck, *Phys. Rev. Lett.* **71**, 2184 (1993).
- [4] H. F. Beyer, *IEEE Trans. Instrum. Meas.* **44**, 510 (1995); H. F. Beyer, G. Menzel, D. Liesen, A. Gallus, F. Bosch, R. Deslattes, P. Indelicato, Th. Stöhlker, O. Klepper, R. Moshhammer, F. Nolden, H. Eickhoff, B. Franzke, and M. Steck, *Z. Phys. D* **35**, 169 (1995).
- [5] D. Liesen, H. F. Beyer, and G. Menzel, *Comments At. Mol. Phys.* **32**, 23 (1995).
- [6] G. E. Brown, J. S. Langer and G. W. Schaefer, *Proc. Roy. Soc. London A* **251**, 92 (1959).
- [7] A. M. Desiderio and W. R. Johnson, *Phys. Rev. A* **3**, 1267 (1971).
- [8] P. J. Mohr, *Ann. Phys. (N.Y.)* **88**, 26 (1974).
- [9] P. J. Mohr, *Phys. Rev. Lett.* **34**, 1050 (1982).
- [10] N. J. Snyderman, *Ann. Phys. (N.Y.)* **211**, 43 (1991).
- [11] S. A. Blundell and N. J. Snyderman, *Phys. Rev. A* **44**, 1427 (1991).
- [12] H. Persson, I. Lindgren, and S. Salomonson, *Phys. Scr.* **T46**, 125 (1993); I. Lindgren, H. Persson, S. Salomonson, and A. Ynnermann, *Phys. Rev. A* **47**, 4555 (1993).



- [13] H. M. Quiney and I. P. Grant, *J. Phys. B* **27**, L199 (1994).
- [14] E. H. Wichmann and H. M. Kroll, *Phys. Rev.* **101**, 843 (1956).
- [15] G. Soff and P. J. Mohr, *Phys. Rev. A* **38**, 5066 (1988).
- [16] H. Persson, I. Lindgren, S. Salomonson, and P. Sunnergren, *Phys. Rev. A* **48**, 2772 (1993).
- [17] W. R. Johnson, S. A. Blundell, and J. Sapirstein, *Phys. Rev. A* **37**, 307 (1988).
- [18] S. Salomonson and P. Öster, *Phys. Rev. A* **41**, 4670 (1989).
- [19] A. Mitrushenkov, L. Labzowsky, I. Lindgren, H. Persson, and S. Salomonson, *Phys. Lett. A* **200**, 51 (1995).
- [20] L. Labzowsky, V. Karasiev, I. Lindgren, H. Persson, and S. Salomonson, *Phys. Scr.* **T46**, 150 (1993).
- [21] L. Labzowsky and A. Mitrushenkov, *Phys. Lett. A* **198**, 333 (1995).
- [22] I. Lindgren (unpublished).
- [23] N. L. Manakov and A. A. Nekipelov (unpublished).
- [24] G. Källén and A. Sabry, *Mat. Fys. Medd. Dan. Vid. Selsk.* **29**, 17 (1955).
- [25] T. Beier and G. Soff, *Z. Phys. D* **8**, 129 (1988).
- [26] S. M. Schneider, W. Greiner, and G. Soff, *J. Phys. B* **26**, L529 (1993).
- [27] I. Lindgren, H. Persson, S. Salomonson, V. Karasiev, L. Labzowsky, A. Mitrushenkov, and M. Tokman, *J. Phys. B* **26**, L503 (1993).
- [28] G. Plunien, B. Müller, W. Greiner, and G. Soff, *Phys. Rev. A* **43**, 5853 (1991).
- [29] G. Plunien and G. Soff, *Phys. Rev. A* **53**, 4614 (1996).
- [30] A. N. Artemyev, V. M. Shabaev, and V. A. Yerokhin, *Phys. Rev. A* **52**, 1884 (1995).
- [31] R. Karplus and N. M. Kroll, *Phys. Rev.* **77**, 536 (1950); R. Barbieri, J. A. Mignaco, and E. Remiddi, *Nuovo Cim.* **6A**, 21 (1971); B. E. Lautrup, A. Peterman, and E. de Rafael, *Phys. Rep.* **3C**, 196 (1972).
- [32] M. I. Eides, H. Grotch and D. A. Owen, *Phys. Lett. B* **294**, 115 (1992); M. I. Eides and H. Grotch, *Phys. Lett.* **B301**, 127 (1993); **B308**, 389 (1993); M. I. Eides, H. Grotch, and P. Peller, *Phys. Rev. A* **50**, 144 (1994).
- [33] K. Pachucki, *Phys. Rev. A* **48**, 2609 (1993); K. Pachucki, *Phys. Rev. Lett.* **72**, 3154 (1994).
- [34] J. B. French and V. Weisskopf, *Phys. Rev.* **75**, 1240 (1949).
- [35] H. Persson, Ph.D. thesis, Gothenburg University, 1993 (unpublished).
- [36] N. N. Bogoljubov and D. V. Shirkov, *Introduction to the Theory of Quantized Fields* (Interscience, New York, 1959).
- [37] M. Baranger, F. J. Dyson, and E. E. Salpeter, *Phys. Rev.* **88**, 680 (1952).
- [38] W. R. Johnson and G. Soff, *At. Data and Nucl. Data Tables* **33**, 405 (1985).
- [39] T. Franosch and G. Soff, *Z. Phys. D* **18**, 219 (1991).
- [40] P. J. Mohr, *Phys. Rev. A* **46**, 4421 (1992).
- [41] P. J. Mohr and G. Soff, *Phys. Rev. Lett.* **70**, 158 (1993).
- [42] J. R. Sapirstein and D. R. Yennie, in *Quantum Electrodynamics*, edited by T. Kinoshita (World Scientific, Singapore, 1990), p. 560.
- [43] A. Ynnerman, J. James, I. Lindgren, H. Persson, and S. Salomonson, *Phys. Rev. A* **50**, 4671 (1994).
- [44] L. Labzowsky and M. Tokman, *J. Phys. B* **28**, 3717 (1995).
- [45] S. Blundell, *Phys. Rev. A* **46**, 3762 (1992).
- [46] S. Mallampalli and J. Sapirstein (unpublished).